

Regularized strategies for material parameter identification in the context of finite strain plasticity

A. V. Shutov, R. Kreißig

We analyze the problem of material parameter identification for a certain model of finite strain plasticity/viscoplasticity. The material model takes into account both nonlinear isotropic and kinematic hardening. The nonlinear kinematic hardening of Armstrong-Frederick type is modeled on the grounds of the double multiplicative split of the deformation gradient, which was proposed by Lion.

From the mathematical viewpoint, the parameter identification problem is, in general, ill-conditioned, since the solution does not depend continuously on the input data. Numerical difficulties arise especially when the problem exhibits a strong correlation among the parameters. Thus, a challenge lies in developing regularized identification strategies which reduce the correlation between the parameters and the probability of getting trapped in a local minimum of the objective function. Moreover, a reliable parameter identification strategy should be robust with respect to small measurement errors.

We discuss a regularization technique which involves including additional equality constraints imposed on the material parameters. These constraints are based on mechanical considerations and may contain some additional information about the mechanical response of the material. The mechanical considerations allow to reduce the number of independent parameters and in some cases to reduce the correlation among them. One general guideline for constructing such relations is discussed in the paper: First, some analytical relations are derived in the simplified case of small strains. Next, basing on these simplified results, the relations are generalized to the finite strains.

The efficiency of the regularized approach for the estimation of hardening parameters using the experimental data for EN AW-7075 aluminium alloy processed by equal channel angular extrusion was demonstrated. Although the straight-forward approach results in a good correspondence between the experimental data and the model predictions, the problem of the material parameter identification is not a trivial one. In particular, the error functional exhibits numerous stationary points. It is shown that the use of the regularized strategies allows to reduce the number of parameters being identified, and in some cases to avoid the problem of multiple stationary points.

1 Introduction

The most important requirements that are placed upon the phenomenological material models are as follows:

- accuracy of description of the real material response,
- stability and robustness of the corresponding numerical algorithms,
- possibility of reliable identification of material parameters.

These three requirements are not mutually exclusive but rather complementary to each other. In this paper we analyze the material model of finite strain viscoplasticity (Shutov and Kreißig, 2008b). This model takes both nonlinear isotropic and kinematic hardening into account in a thermodynamically consistent way. Moreover, as it was shown in Shutov et al. (2009), the case of isotropic softening can be covered as well. The accuracy and robustness

of the local time integration algorithms were numerically tested in Shutov and Kreißig (2008b). Some theoretical results concerning the accuracy, stability, and the error accumulation are presented in Shutov and Kreißig (2010) for a simplified version of the material model.

In the current paper we deal with some aspects of the material parameter identification. The main difficulties associated to the parameter identification on the ground of minimization of a certain least-square functional are as follows:

- the majority of optimization procedures can not distinct between global and local minima,
- correlation among the parameters,
- several parameters must be identified simultaneously due to the coupling effects,¹
- in general, there is no continuous dependence of the resulting solution on the input data (ill-posed problem).

The main aim of the current study is to reduce the number of material parameters being identified. As this takes place, the correlation among the remaining parameters must stay within the admissible range.²

Following the conventional approach, the parameter identification problem is reduced to the minimization of some least-squares functional (error functional)

$$\vec{p} = \arg \min_{\vec{p} \in P} \Phi(\vec{p}), \quad (1)$$

where $\vec{p} = (p_1, \dots, p_n)$ stands for the vector of material parameters, the set $P \subseteq \mathbb{R}^n$ represents the set of admissible parameters. The error functional represents the discrepancy between the measurements data and corresponding model predictions (Mahnken and Stein, 1996; Kreißig et al., 2007)

$$\Phi(\vec{p}) = \sum_i (\text{Model prediction}_i(\vec{p}) - \text{Measured data}_i)^2. \quad (2)$$

In order to reduce the number of material parameters, m additional equality constraints can be introduced ($m \leq n$)

$$\vec{g}(\vec{p}) = (g_1, \dots, g_m)(\vec{p}) = 0. \quad (3)$$

We suppose that the set $\mathfrak{M} := \{\vec{p} \in P : \vec{g}(\vec{p}) = 0\}$ is a smooth $(n - m)$ -dimensional manifold and there exists a smooth mapping $\vec{p} = \vec{p}(\vec{P})$, where $\vec{P} \in \mathbb{R}^{n-m}$ is an $(n - m)$ -dimensional vector. More precisely, we suppose that the overall manifold \mathfrak{M} can be covered by a single smooth homeomorphism³

$$\vec{p} : \vec{P} \in \mathfrak{P} \mapsto \vec{p}(\vec{P}) \in \mathfrak{M}, \quad (4)$$

where \mathfrak{P} is an open subset of \mathbb{R}^{n-m} (cf. Figure 1.).

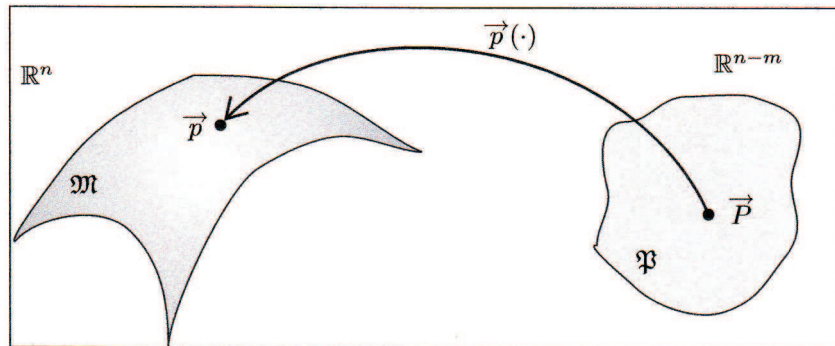


Figure 1. The mapping $\vec{p} : \vec{P} \in \mathfrak{P} \mapsto \vec{p}(\vec{P}) \in \mathfrak{M}$.

¹In particular, since the isotropic and kinematic hardening effects are strongly coupled, the corresponding material parameters should be identified simultaneously.

²In this paper the correlation is estimated using the correlation matrix which contains the information about the first derivatives of the residuals with respect to the parameters (Beck and Arnold, 1977).

³A smooth function f is called a smooth homeomorphism if its inverse f^{-1} exists and is smooth.

Along with the standard minimization problem (1) we consider a restricted one

$$\vec{p} = \arg \min_{\vec{p} \in P, \text{ s.t. } \vec{g}(\vec{p})=0} \Phi(\vec{p}) = \arg \min_{\vec{p} \in \mathfrak{M}} \Phi(\vec{p}). \quad (5)$$

Obviously, if we take the mapping $\vec{p} = \vec{p}(\vec{P})$ into account, the minimization problem (5) is equivalent to

$$\vec{P} = \arg \min_{\vec{P} \in \mathfrak{P}} \Phi(\vec{p}(\vec{P})). \quad (6)$$

Instead of identifying n parameters in (5), only $n - m$ parameters must be determined in (6). In that sense, the number of the parameters is reduced.

We note that constraints (3), independently of the error functional Φ , may contain a certain additional information concerning the mechanical response. For instance, that can be constraints on the saturation stresses, evolution of the size of the elastic domain, or the magnitude of the critical elongation (defined by the onset of the stress softening and localization of deformation). As it will be shown in the following, the introduction of additional constraints can essentially enhance the feasibility of the resulting set of material parameters. On the other hand, the constraints (3) must admit a smooth homeomorphism $\vec{p} = \vec{p}(\vec{P})$ in order to allow for the reduction of the material parameters number. Moreover, in order to solve practical problems, some robust and efficient procedures for computing $\vec{p}(\vec{P})$ are required.

Apparently, any identification procedure with fixing some of the parameters can be considered as a trivial example of such approach.⁴ Some experimentally motivated constraints were introduced in Lion et al. (2008) in order to simplify the parameter identification for a material model of viscoelasticity. Particularly, $2N+1$ constants describing a relaxation spectrum were calculated using three parameters only.

We note that the introduction of some additional equality constraints may have a regularizing effect even without computing the function $\vec{p}(\vec{P})$. Such constrained problem can be solved, for instance, using the method of Lagrange multipliers or its generalizations like the method of sequential quadratic programming (Stoer, 1985). However, in this paper we consider the equality constraints (3) in the context of simplifying the problem by reducing the number of parameters.

In order to avoid a possible ambiguity concerning the use of the terminology, we must remark that different approaches to the "regularization" of an inverse problem exist. In Tikhonov and Arsenin (1977), for instance, a powerful regularization technique for ill-posed inverse problems was considered. This technique is based on the introduction of the so-called regularized operator such that the solution of the regularized problem becomes stable with respect to small changes of the input data (measurements).

In this work a relatively simple problem was analyzed. Thus, only four hardening parameters were identified using experiments with homogeneous deformations. Nevertheless, the discussed methodology can be applied to the parameter identification basing on a series of experiments of different types, including experiments with inhomogeneous loadings (Mahnken and Stein, 1996).

2 Experimental data

Let us analyze the mechanical behavior of the EN AW-7075 aluminium alloy processed by equal channel angular pressing (ECAP) (a general overview concerning the ECAP is presented by Segal (1999)). The experimental setup and the measurements data for the material after four ECAP extrusions (route E) were reported previously in the paper Shutov et al. (2009). In this section we briefly discuss the experimental results which are used for the phenomenological description of the material behavior. The reader, who is interested in details concerning the micromechanical characterization of the material is referred to Shutov et al. (2009).

All experiments were conducted at room temperature. Firstly, a series of strain-controlled tension tests was performed with strain rate ranging from 10^{-4} s^{-1} to 10^2 s^{-1} . No clear rate-dependence of the material response could be identified in that range. Moreover, only quasi-static loadings are considered in the following.

⁴For instance, the initial yield stress can be determined directly by evaluating the flow curve (graphical method).

We note that during ECAP a strong plastic anisotropy can be introduced. In order to analyze the initial anisotropy effects, a series of compression specimens was extracted from the ECAP-processed billet in three mutually orthogonal directions: the extrusion direction, the normal direction, and the transverse direction. No significant discrepancy was observed between the results of uniaxial compression tests for these three kinds of samples (Shutov et al., 2009).

2.1 Monotonic tension and compression tests

In Figure 2, the stress-strain curves corresponding to uniaxial monotonic tension and compression are presented (the specimens were extracted in the extrusion direction from the ECAP-processed billet).

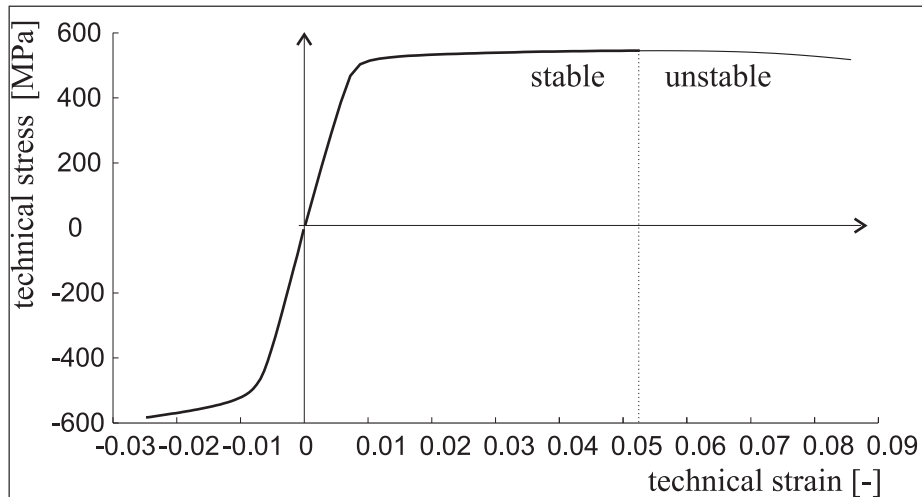


Figure 2. Experimental results: Monotonic tension and compression tests.

We note that the flow stress under tension is approximately the same as under compression (cf. Figure 2). In other words, no significant strength difference effect is observed. Next, the technical stress reaches a maximum at some critical strain level $\varepsilon_{cr} \approx 0.052$. Since the stress response beyond that level is unstable, the homogeneous deformation of the sample can not be guaranteed due to the eventual strain localization in a necked region. Therefore, we use the measurements data only up to that critical strain level.

Although the technical strains do not exceed 10 percent in this experiment, the difference between the stress response in tension and compression can be interpreted as a geometrically nonlinear effect.

2.2 Cyclic tension-compression tests

The quasistatic stress-strain response under uniaxial cyclic strain-controlled loading is presented in Figure 3 for two different experiments.

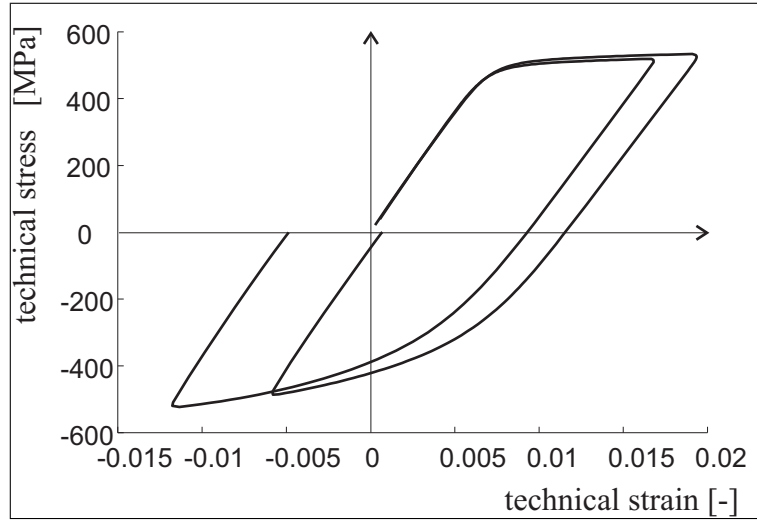


Figure 3. Experimental results: Tension-compression tests.

Note that during the tension phase the tensile yield strength increases, while the yield strength of the material under compression grows smaller (Bauschinger effect). Moreover, the size of the elastic domain is substantially reduced (isotropic softening). Taking into account that the hardening behavior of the material is nonlinear, we conclude that the phenomenological description of the material response should be based on a material model of plasticity which takes a nonlinear kinematic hardening as well as a nonlinear isotropic softening into account.

3 Material model of finite strain viscoplasticity

3.1 Constitutive equations

In this subsection we discuss a material model of finite strain visoplasticity (see Shutov and Kreißig (2008b))⁵. The rheological motivation of the model is presented in Figure 4a. This rheological interpretation motivates the double multiplicative decomposition (cf. the diagram in Figure 4b)⁶

$$\mathbf{F} = \hat{\mathbf{F}}_e \mathbf{F}_i, \quad \mathbf{F}_i = \check{\mathbf{F}}_{ie} \mathbf{F}_{ii}. \quad (7)$$

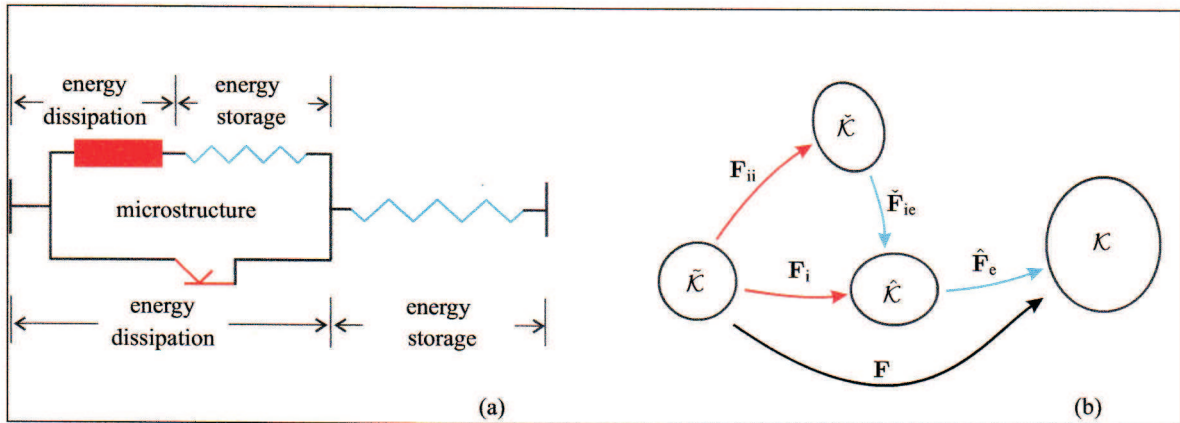


Figure 4. Modeling of kinematic hardening: (a): Rheological model, (b) Commutative diagram showing corresponding configurations with transformations of material line elements.

Firstly, the deformation gradient \mathbf{F} is decomposed into the elastic and the inelastic parts. This decomposition is motivated by the idea of a local elastic unloading.⁷ The second split was proposed by Lion (see Lion (2000),

⁵A similar model of finite strain plasticity was proposed in Vladimirov et al. (2008).

⁶As it was formulated by Rabotnov (1980): The use of rheological models as a guideline in constructing constitutive equations allows for ensuring the thermodynamic consistency in a natural way.

⁷On the other hand, decomposition (7)₁ can be derived from the concept of material isomorphism (see Bertram (2005)).

Helm (2001)) in order to represent the nonlinear kinematic hardening of Armstrong-Frederick type. The tensor $\tilde{\mathbf{F}}_{ic}$ is related to local elastic deformations induced by strong inhomogeneities of dislocations. Along with the well-known right Cauchy-Green tensor $\mathbf{C} = \mathbf{F}^T \mathbf{F}$, we introduce two tensor-valued internal variables

$$\mathbf{C}_i = \mathbf{F}_i^T \mathbf{F}_i, \quad \mathbf{C}_{ii} = \mathbf{F}_{ii}^T \mathbf{F}_{ii}. \quad (8)$$

These variables are interpreted respectively as inelastic right Cauchy-Green tensor and inelastic right Cauchy-Green tensor of microstructure. The material (or Lagrangian) description is used in this paper to formulate the material model.⁸

For a given deformation history $\mathbf{C}(t)$, the material response in the time interval $t \in [0, T]$ is governed by the following system of ordinary differential and algebraic equations with respect to $\mathbf{C}_i(t)$, $\mathbf{C}_{ii}(t)$, $s(t)$, $s_d(t)$, $\lambda_i(t)$

$$\dot{\mathbf{C}}_i = 2 \frac{\lambda_i}{\mathfrak{F}} (\mathbf{C} \tilde{\mathbf{T}} - \mathbf{C}_i \tilde{\mathbf{X}})^D \mathbf{C}_i, \quad \mathbf{C}_i|_{t=0} = \mathbf{C}_i^0, \quad \det \mathbf{C}_i^0 = 1, \quad \mathbf{C}_i^0 \in Sym, \quad (9)$$

$$\dot{\mathbf{C}}_{ii} = 2 \lambda_i \varkappa (\mathbf{C}_i \tilde{\mathbf{X}})^D \mathbf{C}_{ii}, \quad \mathbf{C}_{ii}|_{t=0} = \mathbf{C}_{ii}^0, \quad \det \mathbf{C}_{ii}^0 = 1, \quad \mathbf{C}_{ii}^0 \in Sym, \quad (10)$$

$$\dot{s} = \sqrt{\frac{2}{3}} \lambda_i, \quad \dot{s}_d = \frac{\beta}{\gamma} \dot{s} R, \quad s|_{t=0} = s^0, \quad s_d|_{t=0} = s_d^0, \quad (11)$$

$$\tilde{\mathbf{T}} = 2 \rho_R \frac{\partial \psi_{el}(\mathbf{C} \mathbf{C}_i^{-1})}{\partial \mathbf{C}} \Big|_{\mathbf{C}_i = \text{const}}, \quad \tilde{\mathbf{X}} = 2 \rho_R \frac{\partial \psi_{kin}(\mathbf{C}_i \mathbf{C}_{ii}^{-1})}{\partial \mathbf{C}_i} \Big|_{\mathbf{C}_{ii} = \text{const}}, \quad (12)$$

$$R = \gamma s_e, \quad s_e = s - s_d, \quad (13)$$

$$\lambda_i = \frac{1}{\eta} \left\langle \frac{1}{k_0} f \right\rangle^m, \quad f = \mathfrak{F} - \sqrt{\frac{2}{3}} [K + R], \quad \mathfrak{F} = \sqrt{\text{tr}[(\mathbf{C} \tilde{\mathbf{T}} - \mathbf{C}_i \tilde{\mathbf{X}})^D]^2}. \quad (14)$$

Here, $(\cdot)^D$ stands for a deviatoric part of a second-rank tensor. The material parameters $\rho_R > 0$, $\varkappa \geq 0$, $\beta \geq 0$, $\gamma \in \mathbb{R}$, $\eta \geq 0$, $m \geq 1$, $K > 0$, and the isotropic real-valued functions ψ_{el} , ψ_{kin} are assumed to be known. The constant $k_0 = 1$ MPa is used to get a dimensionless term in the bracket (not a material parameter).

The functions $s(t)$, $s_d(t)$, $\lambda_i(t)$ are interpreted respectively as inelastic arc length, dissipative part of inelastic arc length, and inelastic multiplier. The quantities \mathbf{C} , \mathbf{C}_i , \mathbf{C}_{ii} , s , and s_d uniquely define the 2nd Piola-Kirchhoff tensor $\tilde{\mathbf{T}}(t)$, the backstress tensor $\tilde{\mathbf{X}}(t)$, the isotropic hardening $R(t)$, the overstress $f(t)$, and the norm of the driving force $\mathfrak{F}(t)$.

The above definitions imply that \mathbf{C} and \mathbf{C}_i are symmetric. Since functions ψ_{el} and ψ_{kin} are isotropic, *it makes no difference* whether the derivatives in (12) are interpreted as general derivatives or as derivatives with respect to a symmetric tensor (see, for instance, the discussion in Shutov and Kreißig (2008a)).

In the following we will use a concrete ansatz for ψ_{el} , ψ_{kin} (Helm, 2001)

$$\rho_R \psi_{el}(\mathbf{C} \mathbf{C}_i^{-1}) = \frac{k}{2} (\ln \sqrt{\det \mathbf{C} \mathbf{C}_i^{-1}})^2 + \frac{\mu}{2} (\text{tr} \overline{\mathbf{C} \mathbf{C}_i^{-1}} - 3), \quad \rho_R \psi_{kin}(\mathbf{C}_i \mathbf{C}_{ii}^{-1}) = \frac{c}{4} (\text{tr} \overline{\mathbf{C}_i \mathbf{C}_{ii}^{-1}} - 3), \quad (15)$$

where $k > 0$, $\mu > 0$, $c > 0$ are material constants. The overline $\overline{(\cdot)}$ denotes the unimodular part of a tensor

$$\overline{\mathbf{A}} = (\det \mathbf{A})^{-1/3} \mathbf{A}. \quad (16)$$

Taking the inelastic incompressibility into account ($\det(\mathbf{C}_i) = \det(\mathbf{C}_{ii}) = 1$), we get for stresses and backstresses

$$\tilde{\mathbf{T}} = k \ln \sqrt{\det(\mathbf{C})} \mathbf{C}^{-1} + \mu \mathbf{C}^{-1} (\overline{\mathbf{C} \mathbf{C}_i^{-1}})^D, \quad \tilde{\mathbf{X}} = \frac{c}{2} \mathbf{C}_i^{-1} (\mathbf{C}_i \mathbf{C}_{ii}^{-1})^D. \quad (17)$$

As it was proved in Shutov and Kreißig (2008b), the material model is thermodynamically consistent for $\gamma \geq 0$ (isotropic hardening). The case $\gamma < 0$ (isotropic softening) was covered in Shutov et al. (2009) as well. The reader, who is interested in details concerning the numerical implementation of the material model is referred to Shutov and Kreißig (2008a). The time discretization of the evolution equations is based on so-called geometrical integrators. It was tested numerically in Shutov and Kreißig (2008b) for strain-controlled processes that the use of the geometrical integrators allows to avoid the error accumulation. A mathematical explanation of this fact can be found in Shutov and Kreißig (2010).

⁸In Shutov and Kreißig (2008b), the material model was originally formulated in intermediate configurations. Next, in order to simplify the numerical treatment of the evolution equations, the constitutive relations were transformed to the reference configuration.

3.2 Case of small strains

In this subsection we consider a simplified version of the constitutive equations under the assumption of small strains (rotations and displacements may remain finite). The consideration of the simplified case will provide clear insights into the construction of the regularized strategies for parameter identification. Firstly, we suppose

$$\mathbf{C} \rightarrow \mathbf{1}, \quad \mathbf{C}_i \rightarrow \mathbf{1}, \quad \mathbf{C}_{ii} \rightarrow \mathbf{1}. \quad (18)$$

Moreover, we assume in this subsection that there exists a constant $K_0 > 0$ such that for any time instance t we have the following estimation of the flow stress

$$K + R(t) \geq K_0 > 0. \quad (19)$$

For $\mathbf{E} := 1/2(\mathbf{C} - \mathbf{1})$, $\mathbf{E}_i := 1/2(\mathbf{C}_i - \mathbf{1})$, $\mathbf{E}_{ii} := 1/2(\mathbf{C}_{ii} - \mathbf{1})$, and $\Delta := \max(\|\mathbf{C} - \mathbf{1}\|, \|\mathbf{C}_i - \mathbf{1}\|, \|\mathbf{C}_{ii} - \mathbf{1}\|)$ we obtain from (18)

$$\det(\mathbf{C}) = 1 + 2\text{tr}(\mathbf{E}) + O(\Delta^2), \quad \ln(\sqrt{\det(\mathbf{C})}) = \text{tr}(\mathbf{E}) + O(\Delta^2), \quad (20)$$

$$\bar{\mathbf{C}} = \mathbf{1} + 2\mathbf{E}^D + O(\Delta^2), \quad \mathbf{C}^{-1} = \mathbf{1} - 2\mathbf{E} + O(\Delta^2). \quad (21)$$

Here, O stands for "lage-O" Landau symbol. Equation (21)₂ follows immediately from the well-known Neumann series expansion. Moreover, we get

$$\mathbf{C}_i^{-1} = \mathbf{1} - 2\mathbf{E}_i + O(\Delta^2), \quad \mathbf{C}_{ii}^{-1} = \mathbf{1} - 2\mathbf{E}_{ii} + O(\Delta^2), \quad (22)$$

$$(\bar{\mathbf{C}}\mathbf{C}_i^{-1})^D = 2(\mathbf{E} - \mathbf{E}_i)^D + O(\Delta^2), \quad (\mathbf{C}_i\mathbf{C}_{ii}^{-1})^D = 2(\mathbf{E}_i - \mathbf{E}_{ii})^D + O(\Delta^2), \quad (23)$$

$$\tilde{\mathbf{T}} = k\text{tr}(\mathbf{E})\mathbf{1} + 2\mu(\mathbf{E} - \mathbf{E}_i)^D + O(\Delta^2), \quad \tilde{\mathbf{X}} = c(\mathbf{E}_i - \mathbf{E}_{ii})^D + O(\Delta^2). \quad (24)$$

Combining these results with the definition of the driving force \mathfrak{F} (cf. equation (14)₃), we get

$$\mathfrak{F} = \sqrt{\|(\tilde{\mathbf{T}} - \tilde{\mathbf{X}})^D\|^2 + O(\Delta^3)}. \quad (25)$$

Next, it follows from (14) and (19) that $\lambda_i = 0$ for $\mathfrak{F} < \sqrt{\frac{2}{3}}K_0$. On the other hand, it follows from (25) that $\mathfrak{F} \approx \|(\tilde{\mathbf{T}} - \tilde{\mathbf{X}})^D\|$ for $\mathfrak{F} \geq \sqrt{2/3}K_0$, where " \approx " stands for asymptotic equivalence as $\Delta \rightarrow 0$. Thus, we get

$$\frac{\lambda_i}{\mathfrak{F}} \approx \frac{1}{\eta} \left\langle \frac{\|(\tilde{\mathbf{T}} - \tilde{\mathbf{X}})^D\| - \sqrt{2/3}[K + R]}{k_0} \right\rangle^m \frac{1}{\|(\tilde{\mathbf{T}} - \tilde{\mathbf{X}})^D\|}. \quad (26)$$

Furthermore, we rewrite the evolution equations (9), (10) and put corresponding initial conditions

$$\dot{\mathbf{E}}_i = \frac{\lambda_i}{\mathfrak{F}} \left((\tilde{\mathbf{T}} - \tilde{\mathbf{X}})^D + O(\Delta^2) \right), \quad \mathbf{E}_i|_{t=0} = \mathbf{E}_i^0, \quad \text{tr}(\mathbf{E}_i^0) = O(\Delta^2), \quad \mathbf{E}_i^0 \in Sym, \quad (27)$$

$$\dot{\mathbf{E}}_{ii} = \lambda_i \mathfrak{z} \left(\tilde{\mathbf{X}}^D + O(\Delta^2) \right), \quad \mathbf{E}_{ii}|_{t=0} = \mathbf{E}_{ii}^0, \quad \text{tr}(\mathbf{E}_{ii}^0) = O(\Delta^2), \quad \mathbf{E}_{ii}^0 \in Sym. \quad (28)$$

To be definite, we put in the following $\mathbf{E}_i^0 = \mathbf{E}_{ii}^0 = \mathbf{0}$. Finally, the small-strain counterpart of the material model is obtained by neglecting the terms which are $O(\Delta^2)$ in (24), (27), and (28), and by using the approximation (26) for λ_i/\mathfrak{F} . Note that this simplified model corresponds to the well-known classical material model of small strain viscoplasticity (Chaboche and Rousselier (1983a,b)), where the linearized strain tensor $\boldsymbol{\varepsilon}$ and the Cauchy stress tensor $\boldsymbol{\sigma}$ are formally replaced by the Green strain tensor \mathbf{E} and the 2nd Piola-Kirchhoff tensor $\tilde{\mathbf{T}}$, respectively.⁹

⁹In general, such formal substitution can be justified as follows (Korobeinikov, 2000): Any system of constitutive equations, which is valid under the geometrically linear conditions, can be generalized to small strains (finite rotations and displacements are allowed) by formally replacing $(\boldsymbol{\varepsilon}, \boldsymbol{\sigma}, \dot{\boldsymbol{\varepsilon}}, \dot{\boldsymbol{\sigma}})$ by $(\mathbf{E}, \tilde{\mathbf{T}}, \dot{\mathbf{E}}, \dot{\tilde{\mathbf{T}}})$.

3.3 Some analytical solutions

In this subsection we analyze some properties of the material model. As it will be clear from the discussion in following sections, the knowledge of these properties enables the development of regularized strategies of parameter identification.

Firstly, assuming the zero initial conditions for the isotropic hardening R , the accumulated inelastic arclength s and the dissipative part s_d ($s|_{t=0} = 0$, $s_d|_{t=0} = 0$) and integrating the evolution equation (11)₂ for s_d , the well-known Voce hardening rule is restored

$$R = R(s) = \frac{\gamma}{\beta}(1 - e^{-\beta s}). \quad (29)$$

Note that this result is valid both for finite and for small strains.

Next, let us consider a Cartesian coordinate system $\{\mathbf{e}_1, \mathbf{e}_2, \mathbf{e}_3\}$ and assume a monotonic strain-controlled uniaxial loading along \mathbf{e}_1 . Thus, in terms of the linearized strain tensor $\boldsymbol{\varepsilon}$ and the Cauchy stress tensor $\boldsymbol{\sigma}$ we have

$$\boldsymbol{\varepsilon} = \varepsilon \mathbf{e}_1 \otimes \mathbf{e}_1 - \hat{\varepsilon}(\mathbf{e}_2 \otimes \mathbf{e}_2 + \mathbf{e}_3 \otimes \mathbf{e}_3), \quad \boldsymbol{\sigma} = \sigma \mathbf{e}_1 \otimes \mathbf{e}_1, \quad (30)$$

where $\varepsilon = \varepsilon(t)$ is a given monotonic function; $\hat{\varepsilon}$ and σ are unknown. In this subsection we use notation \mathbf{X} for the backstress tensor of the geometrically linear theory (Subsection 3.2). Substituting this relations into the evolution equations from Subsection 3.2, we get for the backstress \mathbf{X}

$$\mathbf{X} = x(s)(\mathbf{e}_1 \otimes \mathbf{e}_1 - 1/2 \mathbf{e}_2 \otimes \mathbf{e}_2 - 1/2 \mathbf{e}_3 \otimes \mathbf{e}_3), \quad x(s) = \sqrt{\frac{2}{3}} \frac{1}{\kappa} (1 - e^{-\sqrt{3/2} c \kappa s}). \quad (31)$$

Moreover, for quasistatic processes we put (by omitting the elastic deformation phase)

$$\|(\boldsymbol{\sigma} - \mathbf{X})^D\| = \sqrt{2/3} [K + R]. \quad (32)$$

Combining this with (29), (30)₂, and (31) we get the axial component σ of the stress tensor under small strain condition:

$$\sigma(s) = K + \frac{\gamma}{\beta}(1 - e^{-\beta s}) + \sqrt{\frac{3}{2}} \frac{1}{\kappa} (1 - e^{-\sqrt{3/2} c \kappa s}). \quad (33)$$

4 Constraints on the material parameters

Suppose that parameters k, μ, K, η , and m are now known (cf. Section 5). We discuss some constraints which can be imposed on the hardening parameters γ, β, κ, c in order to simplify the parameter identification.¹⁰

First, we consider the case of small strains. If the saturation stress σ^{sat} under monotonic uniaxial tension is known, it may be reasonable to consider the constraint as follows

$$\tilde{g}_1(\gamma, \beta, \kappa, c) = 0, \quad \tilde{g}_1(\gamma, \beta, \kappa, c) := \lim_{s \rightarrow \infty} \sigma(s) - \sigma^{sat}, \quad (34)$$

where $\sigma(s)$ is the axial component of the Cauchy stress tensor given by the geometrically linear counterpart of the material model (we drop the dependence of $\sigma(s)$ on parameters to simplify the notation). Substituting the explicit expression (33) into (34), we get

$$K + \frac{\gamma}{\beta} + \sqrt{\frac{3}{2}} \frac{1}{\kappa} - \sigma^{sat} = 0. \quad (35)$$

This relation is equivalent to

$$\kappa = \sqrt{\frac{3}{2}} \frac{1}{\sigma^{sat} - K - \gamma/\beta}. \quad (36)$$

Thus, the hardening parameter κ is represented as a function of the remaining hardening parameters γ, β, c . In general, in the case of finite strains, this relation is not applicable, since it is based on the assumption of small strains. But it can be seen as a simplified approximation for κ as long as the geometrically linear approach yields proper results (Shutov et al., 2009).

¹⁰Obviously, along with the simplifying effect, the consideration of constraints allows for taking additional information on the material behavior into account.

Now let us discuss a generalization of this approach to the finite strain range. Suppose that a technical stress σ_*^{tech} is known at some point $\varepsilon = \varepsilon_*$, where ε stands for the technical strain.¹¹ Consider the constraint as follows

$$g_1(\gamma, \beta, \kappa, c) = 0, \quad g_1(\gamma, \beta, \kappa, c) := \sigma^{\text{tech}}|_{\varepsilon=\varepsilon_*} - \sigma_*^{\text{tech}}, \quad (37)$$

where $\sigma^{\text{tech}}|_{\varepsilon=\varepsilon_*}$ stands for the model prediction of the technical stress. The solution of equation (37)₁ with respect to κ is denoted by

$$\kappa = \kappa_1(\gamma, \beta, c). \quad (38)$$

The dependence of $\kappa_1(\gamma, \beta, c)$ on σ_*^{tech} is omitted in order to simplify the notation. In this work the function $\kappa_1(\gamma, \beta, c)$ is evaluated numerically using the Newton method.¹²

The next type of equality constraints is based on the knowledge of the critical strain ε_{cr} at which the maximal stress is reached (Cauchy stress and technical stress in geometrically linear and nonlinear cases, respectively). Thus, for small strains, we get

$$\tilde{g}_2(\gamma, \beta, \kappa, c) = 0, \quad \tilde{g}_2(\gamma, \beta, \kappa, c) := \frac{d\sigma(\varepsilon)}{d\varepsilon}|_{\varepsilon=\varepsilon_{cr}}, \quad (39)$$

where $\sigma(\varepsilon)$ is a model prediction. Note that such condition under small strain range can be reasonable only if $\gamma < 0$ (isotropic softening). If $\gamma > 0$ (isotropic hardening) then no peak stresses are predicted, and (39) makes no sense. By neglecting elastic strains, a somewhat more simple relation can be obtained

$$\check{g}_2(\gamma, \beta, \kappa, c) = 0, \quad \check{g}_2(\gamma, \beta, \kappa, c) := \frac{d\sigma(s)}{ds}|_{s=\varepsilon_{cr}}. \quad (40)$$

Substituting the explicit expression (33) into (40), and putting $s = \varepsilon_{cr}$, we get

$$\gamma e^{-\beta\varepsilon_{cr}} + \frac{3}{2} c e^{-\sqrt{3/2} c \kappa \varepsilon_{cr}} = 0. \quad (41)$$

Thus,

$$\kappa = \sqrt{\frac{2}{3}} \frac{1}{c\varepsilon_{cr}} \ln \left(-\frac{3c}{2\gamma} e^{\beta\varepsilon_{cr}} \right). \quad (42)$$

Next, we generalize this approach to finite strains. Towards that end we replace the axial component of the Cauchy stress by the technical stress,

$$g_2(\gamma, \beta, \kappa, c) = 0, \quad g_2(\gamma, \beta, \kappa, c) := \frac{d\sigma^{\text{tech}}(\varepsilon)}{d\varepsilon}|_{\varepsilon=\varepsilon_{cr}}. \quad (43)$$

Denote the solution of this equation with respect to κ by κ_2

$$\kappa = \kappa_2(\gamma, \beta, c). \quad (44)$$

The dependence of $\kappa_2(\gamma, \beta, c)$ on ε_{cr} is omitted to simplify the notation. In the following, the function κ_2 is evaluated numerically.

Finally, let us discuss the third type of constraints. Suppose that at some point which is characterized by accumulated plastic strain $s = s_*$, the size of the elastic domain is known (cf. experimental data in Subsection 2.2): $S_* := \sigma_{\text{tension}} - \sigma_{\text{compression}} > 0$. In the case of small strains we can consider

$$g_3(\gamma, \beta) = 0, \quad g_3(\gamma, \beta) := (K + R(s_*)) - 1/2S_*. \quad (45)$$

Substituting (29) for $R(s)$ we obtain

$$\gamma = \gamma_1(\beta), \quad \gamma_1(\beta) := \frac{\beta}{1 - e^{-\beta s_*}} (1/2S_* - K). \quad (46)$$

Note that $\gamma < 0$ for $S_* < 2K$ (isotropic softening). This approach can be easily generalized to cover finite strains as well. However, in this paper we apply such relation for deformed states under relatively small strains only (cf. Section 5). Thus, the estimation (46) is supposed to yield good results in that case.

¹¹In the following we put $\varepsilon_* := \varepsilon_{cr}$, where ε_{cr} stands for the critical deformation (cf. Section 2.1).

¹²For certain finite-strain models it might be possible to obtain an explicit analytical expression for κ , similar to the expression (36). In this paper, however, we use a more general numerical approach.

5 Parameter identification

The elasticity parameters can be identified using the measurements data in elastic range: $\mu = 26300$ MPa, $k = 68600$ MPa. The parameters of the Perzyna-law, for instance, can be obtained basing on the measurements of the overstress f for a series of loading rates. In this paper we neglect the viscous effects by putting $\eta = 0$ s, $m = 1$. Furthermore, the initial flow stress is identified by the qualitative analysis of the flow curve (graphical method): $K = 485$ MPa. In the following we discuss some identification procedures for determining the hardening parameters.

5.1 Straight-forward approach

Four uniaxial experiments are considered in this section: one monotonic tension (cf. Section 2.1) for $\varepsilon \leq \varepsilon_{cr} = 0.052$ ($n_1 = 35$ data points), one monotonic compression (cf. Section 2.1, $n_2 = 43$ data points), and two tension-compression experiments (cf. Section 2.2, $n_3 = 137, n_4 = 152$ data points). Let us denote the experimentally measured technical stresses by $\hat{\sigma}_{k,i}^{\text{tech}}$, where $k \in \{1, 2, 3, 4\}$ stands for the number of the experiment and $i \in \{1, 2, \dots, n_k\}$ for the corresponding measurement point.

Basing on these data, we consider an error functional as follows

$$\Phi(\gamma, \beta, \kappa, c) := \sum_{k=1}^4 \sum_{i=1}^{n_k} (\hat{\sigma}_{k,i}^{\text{tech}} - \sigma_{k,i}^{\text{tech}}(\gamma, \beta, \kappa, c))^2, \quad (47)$$

where $\sigma_{k,i}^{\text{tech}}(\gamma, \beta, \kappa, c)$ stands for the corresponding simulation results.

The error functional Φ is minimized using the Levenberg-Marquardt method (Newton method with damping). Two stationary points \vec{p}_1 and \vec{p}_2 were identified numerically. The corresponding parameter sets are summarized in Table 6. Note that \vec{p}_1 and \vec{p}_2 are adjacent to each other. This illustrates the fact that even having a "very good" initial guess for the solution, the convergence to the global minimum can not be guaranteed.

Since $\Phi(\vec{p}_2)$ is smaller than $\Phi(\vec{p}_1)$ (see Table 6), we consider the set \vec{p}_2 to be the solution of the problem within the straight-forward approach. The corresponding simulation results are plotted in Figure 5. The correlation matrix for \vec{p}_2 is presented in Table 1.

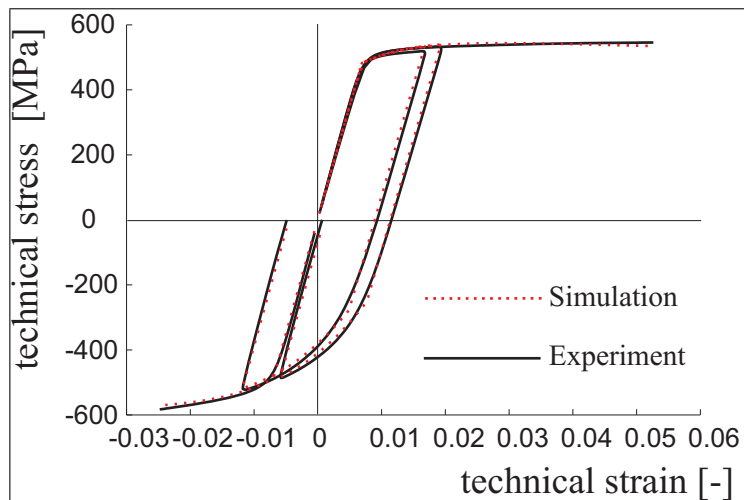


Figure 5. Simulation results for \vec{p}_2 (straight-forward approach).

We see that the parameters β , γ and c are correlated. Nevertheless, the correlation remains in the admissible range. Thus, the parameter identification is possible. On the other hand, since the target function Φ possesses numerous stationary points (at least two), a series of optimization computations is required to get the global minimum of Φ . This circumstance makes the reliable parameter identification especially time consuming, if numerous parameters are to be identified simultaneously.

One important feature of the parameter sets \vec{p}_1 and \vec{p}_2 , which has to be taken into account, is that smaller stresses are predicted by the model under tension and compression near the termination points. The second feature

Table 1: Correlation matrix: straight-forward approach

	β	c	γ	κ
β	1.0	0.58	-0.90	-0.16
c	0.58	1.0	-0.82	-0.27
γ	-0.90	-0.82	1.0	0.37
κ	-0.16	-0.27	0.37	1.0

is that the technical stresses reach their maximum under tension at much smaller strains than in the experiment. In particular, this implies that the onset of unstable deformation (strain localization) occurs at smaller strains.¹³

5.2 Regularized strategies basing on g_1 and g_3

Now let us consider a constrained optimization problem basing on the equality constraint (37). We put in (37) $\varepsilon_* := \varepsilon_{cr} = 0.052$. Thus, we minimize $\Phi_{g_1}(\gamma, \beta, c) := \Phi(\gamma, \beta, \kappa_1(\gamma, \beta, c), c)$. The functional was minimized with respect to γ , β , and c using a series of different initial approximations. The same parameter set \vec{p}_3 is obtained in all cases (no numerous stationary points identified). The correlation matrix is presented in Table 2. Note that the correlation between the parameters remains in the admissible range.

Table 2: Correlation matrix: use of g_1

	β	c	γ
β	1.0	0.80	-0.94
c	0.80	1.0	-0.92
γ	-0.94	-0.92	1.0

Although the identified minimum of the error functional $\Phi(\vec{p}_3)$ is somewhat larger than $\Phi(\vec{p}_2)$ (see Table 6), the stress response is better predicted near the termination points for tension and compression loadings (see Figure 6).

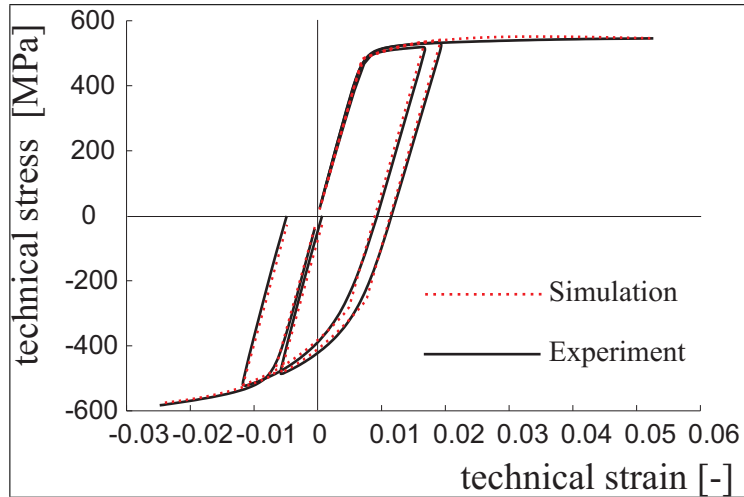


Figure 6. Simulation results for \vec{p}_3 (optimization under use of g_1).

The next strategy is based on the combination of equality constraints (37) and (45). Thus, we minimize now $\Phi_{g_1, g_3}(\beta, c) := \Phi_{g_1}(\gamma_1(\beta), \beta, c) = \Phi(\gamma_1(\beta), \beta, \kappa_1(\gamma_1(\beta), \beta, c), c)$ with respect to β and c . In order to make use of (45), we put in this paper $S_* := 775$ MPa, $s_* := 0.019$. Similarly to the minimization of $\Phi_{g_1}(\gamma, \beta, c)$, only one stationary point \vec{p}_4 is identified. The correlation matrix is presented in Table 3. The simulation results basing on the set \vec{p}_4 are close to that of \vec{p}_3 (see Figure 7).

¹³One possible way of dealing with these problems is to introduce additional terms like $\alpha_1(g_1)^2$ or $\alpha_2(g_2)^2$ into the formulation of the error functional (47), where coefficients α_i should be large enough in order to influence the optimization positively. On the other hand, the problem becomes ill-conditioned for large values of α_i . Thus, the optimal choice of the coefficients α_i is not a trivial task.

Table 3: Correlation matrix: use of g_1 and g_3

	β	c
β	1.0	0.78
c	0.78	1.0

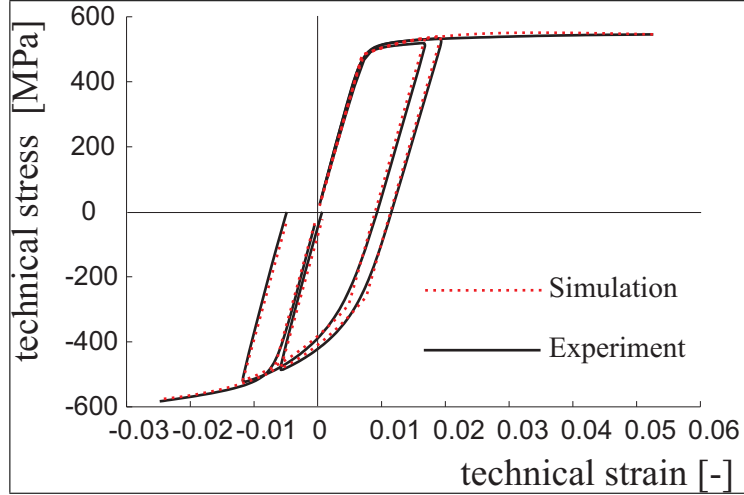


Figure 7. Simulation results for \vec{p}_4 (optimization under use of g_1 and g_3).

Similar to the previous subsection, the common feature of the parameter sets \vec{p}_3 and \vec{p}_4 is that the predicted critical strain is essentially smaller than the experimentally measured one.

5.3 Regularized strategies basing on g_2 and g_3

On the grounds of the constraint (43) we consider now $\Phi_{g_2}(\gamma, \beta, c) := \Phi(\gamma, \beta, \kappa_2(\gamma, \beta, c), c)$. The minimization of Φ_{g_2} yields the parameter vector \vec{p}_5 . Note that $\Phi(\vec{p}_5)$ is larger than $\Phi(\vec{p}_2)$, $\Phi(\vec{p}_3)$, or $\Phi(\vec{p}_4)$. The corresponding simulation result is presented in Figure 8. Apparently, the constraint (43) is *much more restrictive* than the constraints (37) and (45). The use of the constraint (43) can be justified if the correct prediction of the critical strain *has a primary importance*.¹⁴ Note that the correlation between the parameters remains in the admissible range (Table 4).

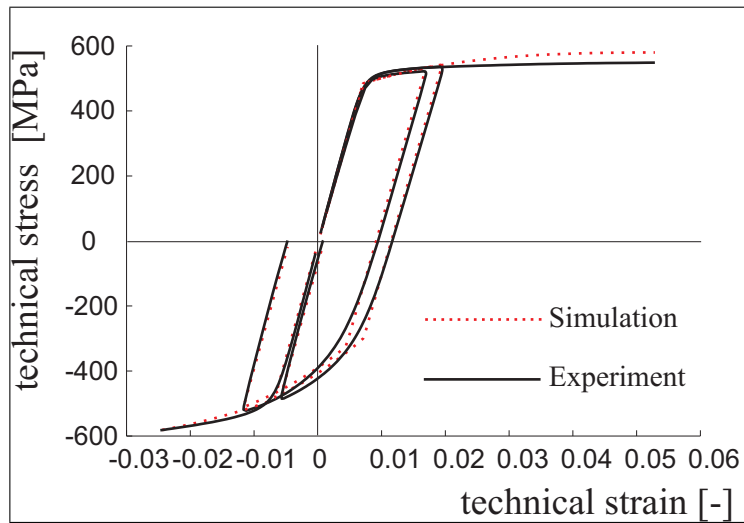


Figure 8. Simulation results for \vec{p}_5 (optimization under use of g_2).

¹⁴Obviously, we are dealing with two conflicting requirements in this case : 1st: minimize $\Phi(\vec{p})$, 2nd: minimize $(g_2(\vec{p}))^2$. In general, such problems should be solved in the context of multi-criteria optimization. However, in this paper the constraints are used at the first place in order to simplify the problem. Therefore, the multi-criteria optimization is not addressed in this study.

Table 4: Correlation matrix: use of g_2

	β	c	γ
β	1.0	0.77	-0.94
c	0.77	1.0	-0.90
γ	-0.94	-0.90	1.0

Finally, if we impose the constraints (43) and (45) on the hardening parameters, we need to minimize $\Phi_{g_2, g_3}(\beta, c) := \Phi_{g_2}(\gamma_1(\beta), \beta, c) = \Phi(\gamma_1(\beta), \beta, \kappa_2(\gamma_1(\beta), \beta, c), c)$. We denote the resulting parameter set by \vec{p}_6 . As it follows from Table 5, the correlation between β and c remains within the admissible range. The corresponding simulation result is depicted in Figure 9. Note that the use of Φ_{g_2, g_3} yields similar results as the ones obtained by the minimization of Φ_{g_2} .

Table 5: Correlation matrix: use of g_2 and g_3

	β	c
β	1.0	0.88
c	0.88	1.0

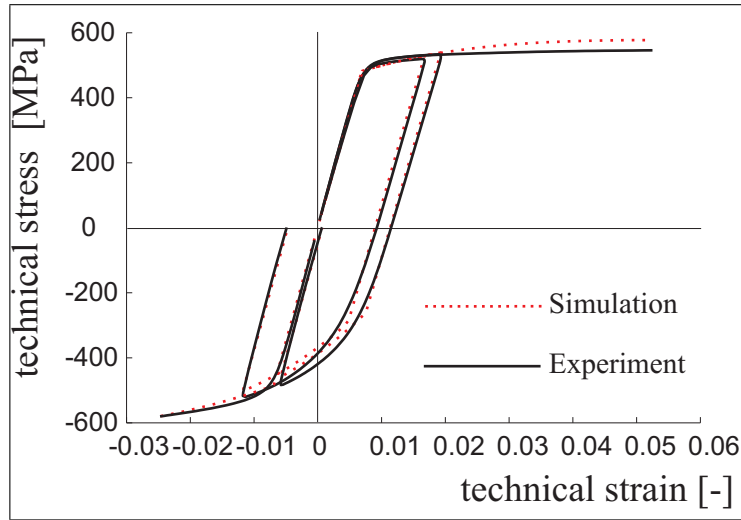


Figure 9. Simulation results for \vec{p}_6 (optimization under use of g_2 and g_3).

Finally, the results of the parameter identification for different identification strategies are summarized in Table 6.

Table 6: Results of parameter identification

	constraints	γ [MPa]	β [-]	κ [MPa ⁻¹]	c [MPa]	$\Phi(\vec{p}_i)$ [MPa ²]
\vec{p}_1		-12805	112.2	0.006377	16370	66421
\vec{p}_2		-14126	121.2	0.006317	17290	66012
\vec{p}_3	$g_1 = 0$	-12977	121.6	0.006226	15560	68527
\vec{p}_4	$g_1 = g_3 = 0$	-13111	122.4	0.006214	15660	68542
\vec{p}_5	$g_2 = 0$	-8921	103.7	0.005658	10890	98859
\vec{p}_6	$g_2 = g_3 = 0$	-12034	108.7	0.005080	12660	118280

6 Conclusion and discussion

One approach to the parameter identification was numerically tested in this paper. The approach is based on the introduction of additional equality constraints during the formulation of minimization problem. The basic principles for choosing these constraints are as follows:

- The constraints should admit a plausible mechanical interpretation.

- The mechanical quantities¹⁵ used to formulate these constraints should be stable with respect to the measurement errors.
- The constraints should depend continuously on the input data.
- The constraints should admit the construction of a smooth homeomorphism $\vec{p} = \vec{p}(\vec{P})$ (cf. (4)).

In this paper we do not analyze mathematically the existence and smoothness of functions $\kappa_1(\gamma, \beta, c)$ (cf. (37)) and $\kappa_2(\gamma, \beta, c)$ (cf. (43)). Instead, we present, basing on a geometrically linear simplification of the model, some explicit analytical solutions (cf. equations (36) and (42)). These analytical solutions can be seen as an approximation for the case of moderate stains. Moreover, the numerical tests indicate that the Newton method allows to solve nonlinear equations (37) and (43) numerically, using results (36) and (42) as initial approximations. In particular, *no computational difficulties* were encountered in evaluating the functions κ_1 and κ_2 . We note that the consideration of the geometrically linear simplification may serve as a guideline in formulating the constraints (and corresponding initial approximations) in the general case of finite strains. Obviously, the construction of reasonable constraints should be based both on the reliable *information* about the real mechanical behavior and the *understanding* of the material model.

As it was shown in the paper, the straight forward approach has three disadvantages: the presence of multiple stationary points, the incorrect prediction of the critical strain ε_{cr} , and underestimated stresses near the termination points under tension and compression (see Figure 5). The introduction of additional constrains allows to reduce the number of material parameters and to achieve a better prediction of the stress response near the termination points. The introduction of additional constraints does not lead to a bad correlation between the material parameters. Since the number of parameter is reduced, the eventual problem of multiple local minima can be dealt in a much simpler way. Moreover, for the example considered in this study, no numerous stationary points were observed for constrained minimization problems.

The requirement of correct prediction of the critical strain ε_{cr} appears to be restrictive for this current example such that $\Phi(\vec{p}_6)$ is almost two times larger than $\Phi(\vec{p}_2)$. On the other hand, the solution \vec{p}_6 is optimal in its class.

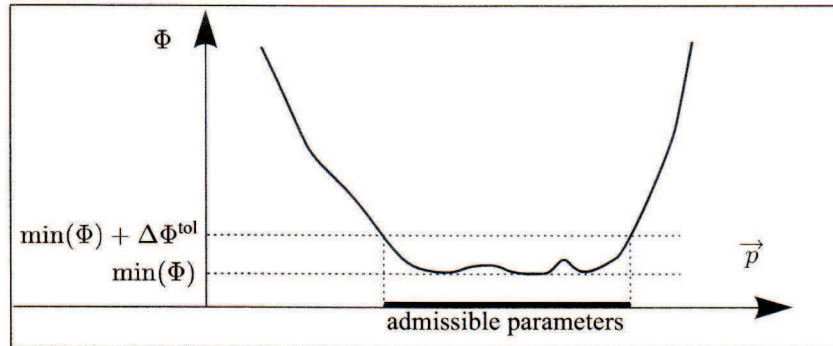


Figure 10. The set of admissible parameters in the context of the toleration condition (48).

In general, the problem of minimizing the error functional is ill-posed, since small changes of input data (experimental results) can lead to finite changes of the solution \vec{p} (resulting parameter vector). In other words, the minimizing vector \vec{p} is not a continuous function of the input data. On the other hand, the experimental data contain some measurement errors. Moreover, some small discrepancy between the real material behavior and the model prediction can be tolerated. Thus, there exists a toleration parameter $\Delta\Phi^{\text{tol}}$, such that all parameters \vec{p}^* satisfying

$$\Phi(\vec{p}^*) \leq \min(\Phi) + \Delta\Phi^{\text{tol}}, \quad (48)$$

should be considered as admissible ones (see Figure 10). A major *challenge* lies in developing identification strategies which fulfil two requirements as follows: (i) the parameters \vec{p}^* must be admissible in the sense of (48), (ii) \vec{p}^* must depend *continuously* on the input data.

We may put, for instance, $\Delta\Phi^{\text{tol}} := \min(\Phi)$. In that case, the results \vec{p}_4 and \vec{p}_6 can be seen as admissible ones (cf. Table 6). Moreover, the corresponding minimization problems (minimization of Φ_{g_1, g_3} and Φ_{g_2, g_3}) are

¹⁵Like the peak stress σ_* or the critical strain ε_{cr} .

advantageous to the straight-forward approach (minimization of Φ) since only one stationary point is observed. Furthermore, relations (36), (42) and (46) depend smoothly on the input data σ^{sat} , ε_{cr} , and S_* , and it was tested numerically that $\kappa_1(\gamma, \beta, c)$ and $\kappa_2(\gamma, \beta, c)$ depend continuously on σ_*^{tech} and ε_{cr} , respectively. Thus, we conclude that the minimization of Φ_{g_1, g_3} and Φ_{g_2, g_3} is a step towards meeting the major challenge mentioned above.

Acknowledgement

This research was supported by German Science Foundation (DFG) within the collaborative research center SFB 692 "High-strength aluminium based light weight materials for reliable components".

References

- Beck, J. V.; Arnold, K. J.: *Parameter Estimation in Engineering and Science*. Wiley, New York (1977).
- Bertram, A.: *Elasticity and Plasticity of Large Deformations*. Springer (2005).
- Chaboche, J. L.; Rousselier, G.: On the plastic and viscoplastic constitutive equations, part 1: Rules developed with internal variable concept. *Journal of Pressure Vessel Technology*, 105, (1983a), 153 – 158.
- Chaboche, J. L.; Rousselier, G.: On the plastic and viscoplastic constitutive equations, part 2: Application of internal variable concept to the 316 stainless steel. *Journal of Pressure Vessel Technology*, 105, (1983b), 159 – 164.
- Helm, D.: *Formgedächtnislegierungen, experimentelle Untersuchung, phänomenologische Modellierung und numerische Simulation der thermomechanischen Materialeigenschaften*. Universitätsbibliothek Kassel, Kassel (2001).
- Korobeinikov, S. N.: *Nonlinear Deformation of Solids [in Russian]*. Izd. Sib. Otd. Ross. Akad. Nauk, Novosibirsk (2000).
- Kreißig, R.; Benedix, U.; Görke, U.; Lindner, M.: Identifikation and estimation of constitutive parameters for material laws in elastoplasticity. *GAMM-Mitteilungen*, 30(2), (2007), 458 – 480.
- Lion, A.: Constitutive modelling in finite thermoviscoplasticity: a physical approach based on nonlinear rheological elements. *International Journal of Plasticity*, 16, (2000), 469 – 494.
- Lion, A.; Yagimli, B.; Baroud, G.; Goerke, U.: Constitutive modelling of pmma-based bone cement: a functional model of viscoelasticity and its approximation for time domain investigations. *Arch. Mech.*, 60 (3), (2008), 221 – 242.
- Mahnken, R.; Stein, E.: A unified approach for parameter identification of inelastic material models in the frame of the finite element method. *Computer Methods in Applied Mechanics and Engineering*, 136, (1996), 225 – 258.
- Rabotnov, I. N.: *Elements of hereditary solid mechanics [Rev. from the 1977 Russian ed.]*. Mir Publishers, Moscow (1980).
- Segal, V. M.: Equal channel angular extrusion: from macromechanics to structure formation. *Materials Science and Engineering*, A271, (1999), 322 – 333.
- Shutov, A. V.; Hockauf, K.; Halle, T.; Kreißig, R.; Meyer, L.: Experimentelle und phänomenologische beschreibung des mechanischen verhaltens der aluminiumlegierung en aw-7075 nach großer plastischer vorverformung. *Materialwissenschaft und Werkstofftechnik*, 40 (7), (2009), 551 – 558.
- Shutov, A. V.; Kreißig, R.: Application of a coordinate-free tensor formalism to the numerical implementation of a material model. *Z. Angew. Math. Mech. (ZAMM)*, 88 (11), (2008a), 888 – 909.
- Shutov, A. V.; Kreißig, R.: Finite strain viscoplasticity with nonlinear kinematic hardening: Phenomenological modeling and time integration. *Computer Methods in Applied Mechanics and Engineering*, 197, (2008b), 2015 – 2029.
- Shutov, A. V.; Kreißig, R.: Geometric integrators for multiplicative viscoplasticity: analysis of error accumulation. *Computer Methods in Applied Mechanics and Engineering*, 199, (2010), 700 – 711.

Stoer, J.: Foundations of recursive quadratic programming methods for solving nonlinear programs. In: K. Schittkowski, ed., *Computational Mathematical Programming, Series F: Computer and Systems Sciences*, NATO ASI Series (1985).

Tikhonov, A. N.; Arsenin, V. A.: *Solution of Ill-posed Problems*. Winston & Sons, Washington (1977).

Vladimirov, I. N.; Pietryga, M. P.; Reese, S.: On the modelling of non-linear kinematic hardening at finite strains with application to springback — comparison of time integration algorithms. *International Journal for Numerical Methods in Engineering*, 75, (2008), 1 – 28.

Address: Dr. Alexey Shutov and Prof. Dr.-Ing. Reiner Kreißig, Institut für Mechanik und Thermodynamik, Technische Universität Chemnitz, D-09111 Chemnitz.
email: alexey.shutov@mb.tu-chemnitz.de.